Earth's normal modes

Séverine Rosat

Institut Terre et Environnement de Strasbourg (ITES)
Université de Strasbourg/EOST, CNRS, Strasbourg, France

July 8, 2021

Introduction

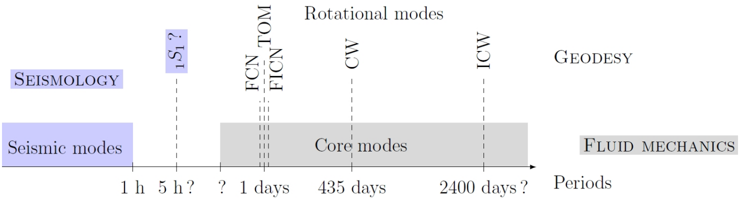

- Seismic modes (elastic feedback)

- Core modes:

– Gravity modes (Archimedean/buoyancy) $\quad {}_1S_1$ **"Slichter" mode**

– Inertial modes (Coriolis)

"core undertones": gravito-inertial modes

– Alfven or hydromagnetic modes (Lorentz)

- Rotational modes (torques): Chandler wobble (CW), Inner Core wobble (ICW), Free Core Nutation (FCN), Free Inner Core Nutation (FICN)

Outline

Undamped harmonic oscillator: mass-spring system

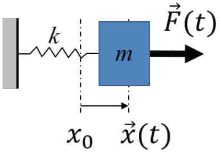

- Tension $\vec{T} = -k(l - l_0)\vec{u}$, where k stiffness, $\vec{u}$ unit vector from fix to mobile (towards point at which the force exerts)
- External force $\vec{F}$

- Fundamental principle of dynamics on mass m: $m\ddot{x}(t) = -kx(t) + F(t)$

$$\ddot{x}(t) + \omega_0^2 x(t) = F(t),$$

where $\omega_0 = \sqrt{\frac{k}{m}}$ is the eigenfrequency of the harmonic oscillator.

- If $F(t) = 0$, the solution to the homogeneous equation is $x(t) = A\cos\omega_0 t + B\sin\omega_0 t$ (A, B constant depending on initial conditions). This is the *normal mode* (free oscillation) of the system.

Undamped harmonic oscillator: mass-spring system

- If $F(t) \neq 0$, the solution of this forced problem consists of the sum of a particular solution with the solution to the homogeneous problem.

- If F is an infinite harmonic (monochromatic) function, $F(t) = F \cos \omega_f t$, then the solution is written:

$$x(t) = \frac{F}{\omega_0^2 - \omega_f^2} \cos \omega_f t$$

The solution is a *forced oscillation*. When $\omega_f = \omega_0$, there is *resonance*.

Damped harmonic oscillator: mass-spring piston system

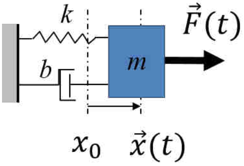

$$m\ddot{x}(t) + b\dot{x}(t) + kx(t) = F(t)$$

b is the *damping coefficient* or *coefficient of friction*.

$$\ddot{x}(t) + 2\alpha\dot{x}(t) + \omega_0^2 x(t) = 0$$

$$Q = \frac{\sqrt{km}}{b} = \frac{\omega_0}{2\alpha} = 2\pi\frac{\text{energy stored}}{\text{energy lost per cycle}}$$

- Overdamped ($\frac{1}{2Q} > 1$): The system returns (exponential decay) to steady state without oscillating.
- Critically damped ($\frac{1}{2Q} = 1$): The system returns to steady state as quickly as possible without oscillating.
- Underdamped ($\frac{1}{2Q} < 1$): The system oscillates at frequency $\omega_0\sqrt{1 - \frac{1}{4Q^2}}$ with amplitude gradually decreasing to zero.

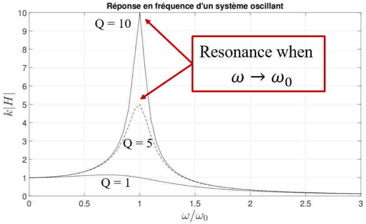

Coupled harmonic oscillators

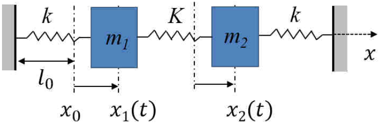

Tension $\vec{T} = -k(l - l_0)\vec{u}$, where k stiffness, $\vec{u}$ unit vector from fix to mobile (towards point at which the force exerts)

- Fundamental principle of dynamics on mass m_1:

$$m_1\ddot{x}_1 = \underbrace{-k(l_0 + x_1 - l_0)}_{\text{on } m_1 \text{ from 1st spring}} \underbrace{-K(l_0 + x_2 - x_1 - l_0) \times (-1)}_{\text{on } m_1 \text{ from } K\text{, -}u_x} = -kx_1 + K(x_2 - x_1)$$

$$\rightarrow m_1\ddot{x}_1 + (k + K)x_1 = Kx_2$$

- on mass m_2: $m_2\ddot{x}_2 = \underbrace{-K(l_0 + x_2 - x_1 - l_0)}_{\text{from 2nd spring K}} \underbrace{-k(l_0 - x_2 - l_0) \times (-1)}_{\text{from 3rd spring}}$

$$m_2\ddot{x}_2 = -K(x_2 - x_1) - kx_2 \rightarrow m_2\ddot{x}_2 + (K + k)x_2 = Kx_1$$

Coupled harmonic oscillators

- Coupled differential system:

$$m_1\ddot{x}_1 + (k+K)x_1 = Kx_2$$
$$m_2\ddot{x}_2 + (k+K)x_2 = Kx_1$$

We assume $m_1 = m_2 = m$. We introduce $\sigma = x_1 + x_2$ and $\delta = x_1 - x_2$.

- The system becomes a system of decoupled differential equations:

$$\begin{cases} \ddot{\sigma} + \frac{k}{m}\sigma = 0, \omega_s = \sqrt{\frac{k}{m}} \text{ pulsation of the symmetric mode} \\ \ddot{\delta} + \frac{k+2K}{m}\delta = 0, \omega_a = \sqrt{\frac{k+2K}{m}} \text{ pulsation of the anti-symmetric mode} \end{cases}$$

Solutions of the form: $\sigma(t) = A\cos\omega_s t + B\sin\omega_s t$ and $\delta(t) = C\cos\omega_a t + D\sin\omega_a t$. The constants can be obtained with given initial conditions.

Coupled harmonic oscillators

Initial conditions: at $t = 0, x_1 = x_0, x_2 = 0$ and $\dot{x_1} = \dot{x_2} = 0$.

We obtain the solutions:

$$x_1(t) = \frac{x_0}{2}\left[\cos\omega_s t + \cos\omega_a t\right]$$
$$x_2(t) = \frac{x_0}{2}\left[\cos\omega_s t - \cos\omega_a t\right]$$

The solution is a **linear combination of the normal modes** of the system.

For a chain of oscillators with M masses, there would be M modes.

Coupled harmonic oscillators

We assume $K \ll k$ (weak coupling). $\omega_s + \omega_a \approx \omega_s$
$\omega_a - \omega_s = \sqrt{(k+2K)/m} - \sqrt{k/m} = \sqrt{k/m}\left(\sqrt{2K/k} - 1\right) \approx \omega_s K/k$,
$\omega_s K/k \ll \omega_s$.

The system can be written:

$$x_1(t) = x_0 \cos\left(\frac{\omega_s + \omega_a}{2} t\right) \cos\left(\frac{\omega_a - \omega_s}{2} t\right)$$

$$\approx x_0 \cos(\omega_s t) \cos\left(\omega_s \frac{K}{k} t\right)$$

$$x_2(t) = x_0 \sin\left(\frac{\omega_s + \omega_a}{2} t\right) \sin\left(\frac{\omega_a - \omega_s}{2} t\right)$$

$$\approx x_0 \sin(\omega_s t) \sin\left(\omega_s \frac{K}{k} t\right)$$

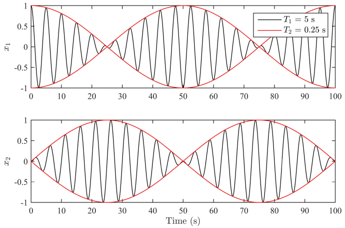

Example of *beating* between two modes

Coupling: We have a transfer of energy between the two modes.

Summary

- A normal mode is the way a system oscillates, given initial conditions.
- The signal is harmonic (a spectral peak at the frequency of the mode), the frequency and damping depend on the properties of the system.
- The normal modes represent a **decomposition basis** for any vibrating system.
- A **coupling** is a transfer of energy between two oscillators.

Table of Contents

History

- theoretical analysis of Earth's eigenmodes by Poisson (1829) but equations were incomplete

- first numerical estimate of the frequency of a free oscillation by Lord Kelvin (1863) (94 min for a fluid sphere whose only restoring force is mutual gravitation or 69 min for a solid Earth)

- first complete treatment for a non-gravitating sphere by Lamb (1882) in Cartesian coordinates. He distinguished between *vibrations of the first class* (spheroidal modes) and *vibrations of the second class* (toroidal modes). ${}_0S_2$ period of 65 min for a Poisson-solid sphere.

- Chree (1889) introduced spherical coordinates

- Bromwich (1898) found that *self-gravitation* reduce the period of the gravest ${}_0S_2$ mode from 65 to 55 min

- Love (1911) solved the system of equations for a homogeneous elastic, self-gravitating sphere (with implicit radially variable properties λ, μ, ρ)

- Hoskins (1920) and Jeffreys (1924) derived explicitly the general equations

History

- Jeans (1927) was the first to place normal modes in the context of seismology: he showed that the superposition of free oscillations or *standing waves* excited by earthquakes could be regarded as a **superposition of travelling body and surface waves**

- Takeuchi (1950): first numerical integration of radial gravito-elastic equations for a spherical Earth; $\omega = 0$ to determine static degree-2 Love numbers h, k, l of a realistic Earth in good agreement with geophysical observations (fortnightly and monthly tides, Chandler wobble, water-tube tidal tilt)

- first variational calculations of elastic-gravitational eigenfrequencies of a realistic Earth model by Jobert (1956, 1957, 1961), Pekeris & Jarosch (1958) and Takeuchi (1959) (${}_0T_2$ 43.5 min, ${}_0S_2$ 52 min)

- Alterman, Jarosch & Pekeris (1959) recast Takeuchi's radial equations into a system of 1st-order equations (2 eq. for *toroidal* and 6 for *spheroidal modes*)

- Numerical integration codes (like MINEOS, OBANI) by Gilbert et al. (1966), G. Masters etc. (https://geodynamics.org/cig/software/mineos/)

Table of Contents

Equilibrium Earth model

- Earth composed of solid and fluid regions

- Regions separated by non-intersecting, smooth, closed surfaces: *interior boundaries*

- Fluid-solid boundaries are **frictionless**

- Earth initially in a state of mechanical equilibrium

- Cartesian axes $(\vec{x}_1, \vec{x}_2, \vec{x}_3)$ rotating uniformly with diurnal angular velocity $\mathbf{\Omega}$ about origin $\mathbf{O}$ situated at the center of mass

- Position of points or material particles denoted $\mathbf{x}$

Poisson's equation

- Initial density distribution ρ^0 within V
- Initial gravitational potential $\phi^0 = -G \int_V \frac{\rho^{0\prime}}{||\mathbf{x}-\mathbf{x}'||} dV'$
- Initial gravitational field $g^0 = -\boldsymbol{\nabla}\phi^0$

Poisson's equation:

$$\nabla^2\phi^0 = 4\pi G\rho^0$$

Continuity conditions:

$$[\phi^0]_-^+ = 0, [\tilde{\mathbf{n}} \cdot \nabla\phi^0]_-^+ = 0$$

Outside the Earth the potential is harmonic:

$$\nabla^2\phi^0 = 0$$

- In the fluid regions, initial stress is hydrostatic: $\mathbf{T}^0 = -p^0\mathbf{I}$

- In the solid regions, initial stress: $\mathbf{T}^0 = -p^0\mathbf{I} + \tau^0$ (isotropic+deviatoric parts) and pressure $p^0 = -\frac{1}{3}tr(\mathbf{T}^0)$

- Static momentum equation:

$$\boldsymbol{\nabla} \cdot \mathbf{T}^0 = \rho^0 \boldsymbol{\nabla}(\phi^0 + \psi) \tag{1}$$

where

$$\psi = -\frac{1}{2}\left[\Omega^2 x^2 - (\boldsymbol{\Omega} \cdot \mathbf{x})\right]$$

is the centrifugal potential, also written as $\boldsymbol{\nabla}_r \psi = \boldsymbol{\Omega} \times (\boldsymbol{\Omega} \times \mathbf{r})$.
In the fluid regions, eq. (1) reduces to the equation of hydrostatic equilibrium:

$$\boldsymbol{\nabla} p^0 + \rho^0 \boldsymbol{\nabla}\left(\phi^0 + \psi\right) = 0$$

- Traction continuity condition on the boundaries: $[\tilde{\mathbf{n}} \cdot \mathbf{T}^0]_-^+ = 0$, on the outer **free surface** of the Earth: $\tilde{\mathbf{n}} \cdot \mathbf{T}^0 = 0$

Linear perturbations

- Lagrangian description of the motion: position vector $\mathbf{r}(\mathbf{x}, t) = \mathbf{x} + \mathbf{s}(\mathbf{x}, t)$, where $\mathbf{s}$ is the *displacement* of particle $\mathbf{x}$ away from its equilibrium position at time t. $\mathbf{s}$ is a small quantity and we ignore terms of second order in $\mathbf{s}$.

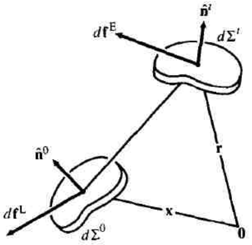

Figure 2.5. The surface forces $d\mathbf{f}^E$ and $d\mathbf{f}^L$ act upon the deformed patch $\hat{\mathbf{n}}^t d\Sigma^t$ at $\mathbf{r}$ and the undeformed patch $\hat{\mathbf{n}}^0 d\Sigma^0$ at $\mathbf{x}$, respectively.

Dahlen & Tromp (1998)

Linear perturbations

- Lagrangian and Eulerian perturbations of quantity q are related by:

$$q^L = q^E + \mathbf{s} \cdot \boldsymbol{\nabla} q^0 \qquad (\leftrightarrow D_t = \partial_t + \mathbf{u}^E \cdot \boldsymbol{\nabla}_r \text{ material derivative})$$

The 1st order change q^{L1} experience by an observer riding on a moving particle consists of the change q^{E1} at a fixed point x in space, plus the change $\mathbf{s} \cdot \boldsymbol{\nabla} q^0$ due to the displacement $\mathbf{s}$ of the particle through the initial spatial gradient $\boldsymbol{\nabla} q^0$.
$\boldsymbol{\nabla}_r$ is the gradient wrt to the fixed spatial position $\mathbf{r}$.

- $d\mathbf{x} = \mathbf{F}^{-1} \cdot d\mathbf{r}$: $\mathbf{F}$ is the *deformation tensor* that relates a vector $d\mathbf{r}$ in the current deformed configuration to a vector $d\mathbf{x}$ in the initial undeformed configuration. It is a cumulative measurement of the deformation experienced by a small ball of material surrounding a moving particle $\mathbf{x}$.

Conservation of mass

- Continuity equation (Eulerian form): $\partial_t \rho^E + \boldsymbol{\nabla}_{\boldsymbol{r}} \cdot (\boldsymbol{\rho}^{\boldsymbol{E}} \mathbf{u}^{\boldsymbol{E}}) = 0$

- Eulerian and Lagrangian perturbations in density ρ^{E1} and ρ^{L1} are defined by $\rho^E = \rho^0 + \rho^{E1}$, $\rho^L = \rho^0 + \rho^{L1}$

- Linearized continuity equation:

$$\boxed{\rho^{E1} = -\boldsymbol{\nabla} \cdot (\rho^0 \mathbf{s})},$$

$$\text{or } \rho^{L1} = -\rho^0 (\boldsymbol{\nabla} \cdot \mathbf{s}), \rho^{L1} = \rho^{E1} + \mathbf{s} \cdot \boldsymbol{\nabla} \rho^0 \tag{2}$$

correct to 1st order in $||\mathbf{s}||$.

Conservation of momentum

$$\rho^E \left[D_t \mathbf{u}^E + \underbrace{2\boldsymbol{\Omega} \times \mathbf{u}^E}_{\textit{Coriolis}} + \underbrace{\boldsymbol{\Omega} \times (\boldsymbol{\Omega} \times \mathbf{r})}_{\textit{centripetal}} \right] = \boldsymbol{\nabla}_{\boldsymbol{r}} \cdot \mathbf{T}^E + \rho^E \mathbf{g}^E \tag{3}$$

- Linearized momentum equation:

$$\rho^0 \left(\partial_t^2 \mathbf{s} + 2\boldsymbol{\Omega} \times \partial_t \mathbf{s} \right) = \boldsymbol{\nabla} \cdot \mathbf{T}^{E1} - \rho^0 \boldsymbol{\nabla} \phi^{E1} - \rho^{E1} \boldsymbol{\nabla} (\phi^0 + \psi) \text{ or}$$

$$\boxed{\rho^0 \left(\partial_t^2 \mathbf{s} + 2\boldsymbol{\Omega} \times \partial_t \mathbf{s} \right) = \boldsymbol{\nabla} \cdot \mathbf{T}^{PK1} - \rho^0 \boldsymbol{\nabla} \phi^{E1} - \rho^0 \mathbf{s} \cdot \boldsymbol{\nabla}\boldsymbol{\nabla} (\phi^0 + \psi)} \tag{4}$$

- *First Piola-Kirchhoff stress* $\mathbf{T}^{PK}$: measure of the force per unit undeformed area; Cauchy stresses $\mathbf{T}^E$ and $\mathbf{T}^L$ are measures of the force per unit deformed area; $\mathbf{T}^{PK1} = \mathbf{T}^{L1} + \mathbf{T}^0 (\boldsymbol{\nabla} \cdot \mathbf{s}) - (\boldsymbol{\nabla} \mathbf{s})^T \cdot \mathbf{T}^0$

Linearized potential theory

- Poisson's equation:

$$\boxed{\nabla^2 \phi^{E1} = 4\pi G \rho^{E1}}$$

- Potential perturbation:

$$\boxed{\phi^{E1} = -G \int_V \frac{\rho^{0\prime} \mathbf{s}' \cdot (\mathbf{x} - \mathbf{x}')}{||\mathbf{x} - \mathbf{x}'||^3} \, dV'}$$

- Gravity perturbation:

$$\boxed{g^{E1} = -\boldsymbol{\nabla} \phi^{E1} = G \int_V \rho^{0\prime} \mathbf{s}' \cdot \left[\frac{\mathbf{I}}{||\mathbf{x} - \mathbf{x}'||^3} - \frac{3(\mathbf{x} - \mathbf{x}')(\mathbf{x} - \mathbf{x}')}{||\mathbf{x} - \mathbf{x}'||^5} \right] dV'}$$

Elastic constitutive relation

- Stress-strain relation (*Hooke's law*): $\mathbf{T}^{PK1} = \mathbf{\Lambda} : \boldsymbol{\nabla}\mathbf{s}$, $\boldsymbol{\nabla}\mathbf{s}$ is the displacement gradient, $\mathbf{\Lambda}$ is a symmetric fourth-order *elastic tensor*

- For a *hydrostatic* Earth model,
  - $\mathbf{T} = \mathbf{\Gamma} : \boldsymbol{\epsilon}$, with $\Gamma_{ijkl} = (\kappa - \frac{2}{3}\mu)\delta_{ij}\delta_{kl} + \mu(\delta_{ik}\delta_{jl} + \delta_{il}\delta_{jk})$, where κ is the isentropic *incompressibility* or bulk modulus and μ is the *rigidity* or shear modulus.
  - $\mathbf{T}^{PK1} = \mathbf{T}^{L1} - p^0(\boldsymbol{\nabla} \cdot \mathbf{s})\mathbf{I} + p^0(\boldsymbol{\nabla}\mathbf{s})^T$
  - equilibrium condition $\boldsymbol{\nabla}\rho^0 + \rho^0\boldsymbol{\nabla}(\phi^0 + \psi) = \mathbf{0}$,
  - taking the curl $\rightarrow \boldsymbol{\nabla}\rho^0 \times \boldsymbol{\nabla}(\phi^0 + \psi) = \mathbf{0}$,
  - taking the cross-product $\rightarrow \boldsymbol{\nabla}p^0 \times \boldsymbol{\nabla}(\phi^0 + \psi) = \mathbf{0}$.
  - Level surfaces of density ρ^0, pressure p^0 and geopotential $\phi^0+\psi$ coincide.

Boundary conditions

- Kinematic boundary conditions:
• solid-solid boundaries Σ_{SS}: $[\mathbf{s}]_-^+ = \mathbf{0}$, no slip
• fluid-solid boundaries (tangential slip allowed) Σ_{FS}: $[\tilde{\mathbf{n}} \cdot \mathbf{s}]_-^+ = \mathbf{0}$, no separation or inter-penetration

- Dynamic boundary conditions:
• solid-solid boundaries Σ_{SS}: $[\tilde{\mathbf{n}} \cdot \mathbf{T}^{PK1}]_-^+ = \mathbf{0}$
• on the outer free surface ∂V: $\tilde{\mathbf{n}} \cdot \mathbf{T}^{PK1} = \mathbf{0}$
• continuity of traction across any slipping boundary:
$[\tilde{\mathbf{n}} \cdot \mathbf{T}^{PK1} - \boldsymbol{\nabla}^{\Sigma} \cdot (\mathbf{s}\tilde{\mathbf{n}} \cdot \mathbf{T}^{0})]_-^+ = \mathbf{0}$

- Gravitational boundary conditions:
• all boundaries Σ: $[\phi^{E1}]_-^+ = 0$ and $[\tilde{\mathbf{n}} \cdot \boldsymbol{\nabla}\phi^{E1} + 4\pi G\rho^0\tilde{\mathbf{n}} \cdot \mathbf{s}]_-^+ = 0$

Table of Contents

Eigenmodes

Solutions of the gravito-elastic equations are of the form:

$$\mathbf{s}(\mathbf{x}, t) = \mathbf{s}(\mathbf{x})e^{i\omega t},$$

where ω are the angular *eigenfrequencies* of the Earth, and the displacement fields $\mathbf{s}(\mathbf{x})$ are associated *eigenfunctions*.

Transform equations of motion and boundary conditions to the frequency domain using

$$\mathbf{s}(\mathbf{x}, \omega) = \int_{-\infty}^{+\infty} \mathbf{s}(\mathbf{x}, t)e^{-i\omega t}\, dt,$$

making the substitution $\partial_t \leftrightarrow i\omega \rightarrow$ **enables to separate spatial dependency from time dependency**

Eigenmodes

For a non-rotating Earth model, the transformed momentum equation

$$-\omega^2\rho^0\mathbf{s} - \boldsymbol{\nabla}\cdot\mathbf{T}^{PK1} + \rho^0\boldsymbol{\nabla}\phi^{E1} + \rho^0\mathbf{s}\cdot\boldsymbol{\nabla}\boldsymbol{\nabla}\phi^0 = \mathbf{0} \text{ in } V, \tag{5}$$

subject to the boundary conditions

$$\begin{aligned} \tilde{\mathbf{n}}\cdot\mathbf{T}^{PK1} &= \mathbf{0} \text{ on } \partial V, \\ \left[\tilde{\mathbf{n}}\cdot\mathbf{T}^{PK1}\right]_-^+ &= \mathbf{0} \text{ on } \Sigma_{SS}, \\ \left[\tilde{\mathbf{n}}\cdot\mathbf{T}^{PK1} - \boldsymbol{\nabla}^{\Sigma}\cdot(\mathbf{s}\tilde{\mathbf{n}}\cdot\mathbf{T}^0)\right]_-^+ &= \mathbf{0} \text{ on } \Sigma_{FS} \end{aligned}$$

We introduce the integro-differential operator $\mathcal{H}$ so that

$$\boxed{\mathcal{H}\mathbf{s} = \omega^2\mathbf{s}}.$$

The quantities ω^2 and $\mathbf{s}$ are the eigenvalues and associated eigenfunctions of the linear operator $\mathcal{H}$.

SNREI Earth model

SNREI = **s**pherically symmetric, **n**on-**r**otating, perfectly **e**lastic and **i**sotropic ("isotropic": no deviatoric stress and Γ is isotropic) $\Gamma_{ijkl} = (\kappa - \frac{2}{3}\mu)\delta_{ij}\delta_{kl} + \mu(\delta_{ik}\delta_{jl} + \delta_{il}\delta_{jk})$

- System of spherical polar coordinates (r, θ, ϕ) with origin at the center of the SNREI model

- Gravity is radial: $\mathbf{g} = -g\mathbf{r}$ where $g = \dot{\Phi}$.

$$g(r) = \frac{4\pi G}{r^2}\int_0^r \rho' r'^2 \, dr', \Phi(r) = -\frac{4\pi G}{r}\int_0^r \rho' r'^2 \, dr'$$

- Mechanical equilibrium (hydrostatic balance): $p(r) = \int_r^a \rho' g' \, dr'$ with $p(a) = 0$.

PREM Earth model

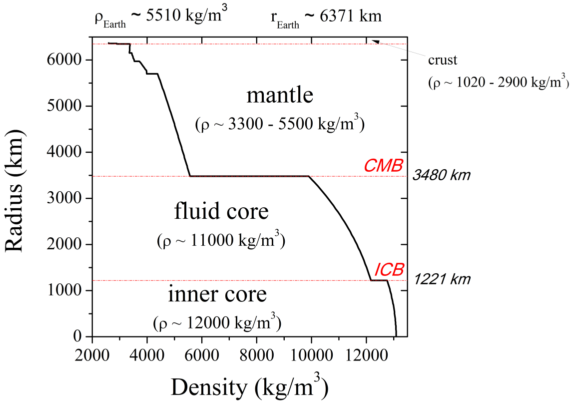

Variation of density with depth in the Preliminary Reference Earth Model (PREM, Dziewonski and Anderson 1981)

PREM Earth model

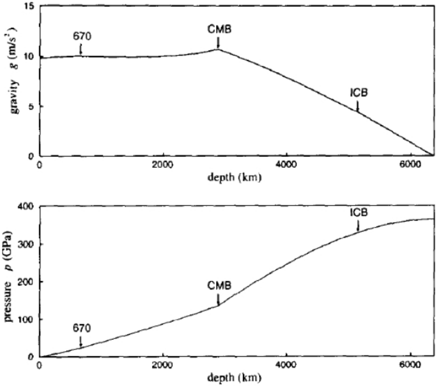

Variation of the acceleration of gravity and hydrostatic pressure with depth in the Preliminary Reference Earth Model (PREM)

[Dahlen and Tromp (1998)]

Radial scalar equations

Equations of motion:

$$
\begin{aligned}
-\omega^2\rho\mathbf{s} - (\kappa + \frac{1}{3}\mu)\boldsymbol{\nabla}(\boldsymbol{\nabla}\cdot\mathbf{s}) - \mu\nabla^2\mathbf{s} - (\dot{\kappa} - \frac{2}{3}\dot{\mu})(\boldsymbol{\nabla}\cdot\mathbf{s})\tilde{\mathbf{r}} \\
-2\dot{\mu}\left[\partial_r\mathbf{s} + \frac{1}{2}\tilde{\mathbf{r}}\times(\boldsymbol{\nabla}\times\mathbf{s})\right] + (4\pi G\rho^2 s_r)\tilde{\mathbf{r}} + \rho\nabla\phi \\
+\rho g\left[\boldsymbol{\nabla}s_r - (\boldsymbol{\nabla}\cdot\mathbf{s} + 2r^{-1}s_r)\tilde{\mathbf{r}}\right] = \mathbf{0}.
\end{aligned}
\tag{6}
$$

Boundary conditions:

$$
\begin{aligned}
\tilde{\mathbf{r}}\cdot\mathbf{T} = \mathbf{0} \text{ on } \partial V, \\
[\tilde{\mathbf{r}}\cdot\mathbf{T}]_-^+ = \mathbf{0} \text{ on } \Sigma_{SS}, \\
[\tilde{\mathbf{r}}\cdot\mathbf{T}]_-^+ = \tilde{\mathbf{r}}[\tilde{\mathbf{r}}\cdot\mathbf{T}\cdot\tilde{\mathbf{r}}]_-^+ = \mathbf{0} \text{ on } \Sigma_{FS}.
\end{aligned}
\tag{7}
$$

Gravitational potential:

$$
\begin{aligned}
\nabla^2\phi = -4\pi G(\rho\boldsymbol{\nabla}\cdot\mathbf{s} + \dot{\rho}s_r) \\
[\phi]_-^+ = 0, \left[\dot{\phi} + 4\pi G\rho s_r\right]_-^+ = 0 \text{ on } \Sigma.
\end{aligned}
\tag{8}
$$

Radial scalar equations

- Earth ≈ sphere → spherical boundary conditions → *spherical harmonics*
- System of spherical polar coordinates (r, θ, ϕ) with origin at the center of the SNREI model
- We seek separable eigensolutions of the form

$$\mathbf{s} = U\mathbf{P}_{lm} + V\mathbf{B}_{lm} + W\mathbf{C}_{lm}, \phi = P\mathcal{Y}_{lm},$$

- The traction is given by

$$\vec{\mathbf{r}} \cdot \mathbf{T} = R\mathbf{P}_{lm} + S\mathbf{B}_{lm} + T\mathbf{C}_{lm},$$

where U, V, W, R, S, T and P are *radial eigenfunctions*.

$$R = (\kappa + \frac{4}{3}\mu)\dot{U} + (\kappa - \frac{2}{3}\mu)r^{-1}(2U - kV),$$

$$S = \mu(\dot{V} - r^{-1}V + kr^{-1}U),$$
$$T = \mu(\dot{W} - r^{-1}W).$$

$\mathcal{Y}_{lm}$ are vector spherical harmonics of degree $0 \leq l \leq \infty$ and order $-l \leq m \leq l$ defined by

$$\mathcal{Y}_{lm}(\theta,\phi) = \left(\frac{2l+1}{4\pi}\right)^{1/2} \frac{1}{2^l l!} \left[\frac{(l-|m|)!}{(l+|m|)!}\right]^{1/2}$$
$$\times (\sin\theta)^{|m|} \left(\frac{1}{\sin\theta}\frac{d}{d\theta}\right)^{l+|m|} (\sin\theta)^{2l}$$
$$\times \begin{cases} \sqrt{2}\cos m\phi & \text{if } -l \leq m < 0 \\ 1 & \text{if } m = 0 \\ \sqrt{2}\sin m\phi & \text{if } 0 < m \leq l \end{cases}$$

$k = \sqrt{l(l+1)}$, $\mathbf{P}_{lm}$, $\mathbf{B}_{lm}$ and $\mathbf{C}_{lm}$ are defined by

$$\mathbf{P}_{lm}(\theta,\phi) = \tilde{\mathbf{r}}\mathcal{Y}_{lm}(\theta,\phi), \mathbf{B}_{lm}(\theta,\phi) = k^{-1}\boldsymbol{\nabla}_1\mathcal{Y}_{lm}(\theta,\phi),$$
$$\mathbf{C}_{lm}(\theta,\phi) = -k^{-1}\left(\tilde{\mathbf{r}}\times\boldsymbol{\nabla}_1\right)\mathcal{Y}_{lm}(\theta,\phi).$$

$\boldsymbol{\nabla}_1 = \vec{\boldsymbol{\theta}}\partial_\theta + \vec{\boldsymbol{\phi}}(\sin\theta)^{-1}\partial_\phi$: surface gradient operator
$\tilde{\mathbf{r}}\times\boldsymbol{\nabla}_1 = -\vec{\boldsymbol{\theta}}(\sin\theta)^{-1}\partial_\phi + \vec{\boldsymbol{\phi}}\partial_\theta$: curl on the unit sphere

Radial scalar equations

Upon substituting the expansions of $\mathbf{s}$ and ϕ into the linearized equation of motion

$\rightarrow$ three second-order ordinary differential equations depending on U, V, W and P.

Radial scalar equations

$$
\begin{aligned}
r^{-2}\frac{d}{dr}\left[r^2\left(\kappa+\frac{4}{3}\mu\right)\dot{U}+\left(\kappa-\frac{2}{3}\mu\right)r(2U-kV)\right]\\
+r^{-1}\left[\left(\kappa+\frac{4}{3}\mu\right)\dot{U}+\left(\kappa-\frac{2}{3}\mu\right)r^{-1}(2U-kV)\right]\\
-3\kappa r^{-1}\left(\dot{U}+2r^{-1}U-kr^{-1}V\right)-k\mu r^{-1}\left(\dot{V}-r^{-1}V+kr^{-1}U\right)+\omega^2\rho U\\
-\rho\left[\dot{P}+\left(4\pi G\rho-4gr^{-1}\right)U+kgr^{-1}V\right]=0
\end{aligned}
$$

$$
\begin{aligned}
r^{-2}\frac{d}{dr}\left[\mu r^2\left(\dot{V}-r^{-1}V+kr^{-1}U\right)\right]+\mu r^{-1}\left(\dot{V}-r^{-1}V+kr^{-1}U\right)\\
+k\left(\kappa-\frac{2}{3}\mu\right)r^{-1}\dot{U}+k\left(\kappa+\frac{1}{3}\mu\right)r^{-2}(2U-kV)\\
+\left[\omega^2\rho-(k^2-2)\mu r^{-2}\right]V-k\rho r^{-1}(P+gU)=0
\end{aligned}
$$

$$
r^{-2}\frac{d}{dr}\left[\mu r^2\left(\dot{W}-r^{-1}W\right)\right]+\mu r^{-1}\left(\dot{W}-r^{-1}W\right)+\left[\omega^2\rho-(k^2-2)\mu r^{-2}\right]W=0
$$

Radial scalar equations

We obtain a second-order ordinary differential equation for the Poisson's equation.

$$\phi^{E1} = -G \int_V \frac{{\rho^0}' \mathbf{s}' \cdot (\mathbf{x} - \mathbf{x}')}{||\mathbf{x} - \mathbf{x}'||^3} dV'$$

$$\ddot{P} + 2r^{-1}\dot{P} - k^2 r^{-2} P = -4\pi G \dot{g} U - 4\pi G \rho \left[\dot{U} + r^{-1}(2U - kV)\right]$$

Associated gravitational boundary conditions

$$[P]_-^+ = 0$$

$$[\dot{P} + 4\pi G \rho U]_-^+ = 0 \text{ on } r = d$$

First-order radial equations

$$\dot{U} = -2(\kappa + \frac{4}{3}\mu)^{-1}(\kappa - \frac{2}{3}\mu)r^{-1}U + k(\kappa + \frac{4}{3}\mu)^{-1}(\kappa - \frac{2}{3}\mu)r^{-1}V + (\kappa + \frac{4}{3}\mu)^{-1}R,$$

$$\dot{V} = -kr^{-1}U + r^{-1}V + \mu^{-1}S,$$

$$\dot{P} = -4\pi G\rho U - (l+1)r^{-1}P + B,$$

$$\dot{R} = [-\omega^2\rho - 4\rho g r^{-1} + 12\kappa\mu(\kappa + \frac{4}{3}\mu)^{-1}r^{-2}]U + \left[k\rho g r^{-1} - 6k\kappa\mu(\kappa + \frac{4}{3}\mu)^{-1}r^{-2}\right]V$$

$$-4\mu(\kappa + \frac{4}{3}\mu)^{-1}r^{-1}R + kr^{-1}S - (l+1)\rho r^{-1}P + \rho B,$$

$$\dot{S} = [k\rho g r^{-1} - 6k\kappa\mu(\kappa + \frac{4}{3}\mu)^{-1}r^{-2}]U - [\omega^2\rho + 2\mu r^{-2} - 4k^2\mu(\kappa + \frac{1}{3}\mu)(\kappa + \frac{4}{3}\mu)^{-1}r^{-2}]V$$

$$-k(\kappa - \frac{2}{3}\mu)(\kappa + \frac{4}{3}\mu)^{-1}r^{-1}R - 3r^{-1}S + k\rho r^{-1}P,$$

$$\dot{B} = -4\pi G(l+1)\rho r^{-1}U + 4\pi Gk\rho r^{-1}V + (l-1)r^{-1}B$$

where $B = \dot{P} + 4\pi G\rho U + (l+1)r^{-1}P$ (to make boundary conditions homogeneous at the surface).

$$\dot{W} = r^{-1}W + \mu^{-1}T,$$

$$\dot{T} = \left[-\omega^2\rho + (k^2 - 2)\mu r^{-2}\right]W - 3r^{-1}T.$$

First-order radial equations

All variables are continuous everywhere in $0 \leq r \leq a$ except for tangential displacement V at fluid-solid boundaries.
$[U]_-^+ = [P]_-^+ = [R]_-^+ = [S]_-^+ = [B]_-^+ = 0$ on $r = d_{SS}$ and $r = d_{FS}$.

$R = S = 0$ and $B = 0$ on $r = a$

The shear traction must vanish on slipping interfaces: $S = 0$ on $r = d_{FS}$

The spherical harmonic development of displacement, tractions and potential is also given in terms of the y_i **system**.

- The displacement

$$\mathbf{s} = U\mathbf{P}_{lm} + V\mathbf{B}_{lm} + W\mathbf{C}_{lm},$$

is also written

$$\mathbf{s} = y_{1,l}\mathbf{P}_{lm} + ry_{3,l}\mathbf{B}_{lm} - y_{7,l}\mathbf{C}_{lm},$$

- The potential $\phi = P\mathcal{Y}_{lm}$ is written $\phi + V = y_{5,l}\mathcal{Y}_{lm}$,

- The traction

$$\vec{\mathbf{r}} \cdot \mathbf{T} = R\mathbf{P}_{lm} + S\mathbf{B}_{lm} + T\mathbf{C}_{lm},$$

is also given by

$$\vec{\mathbf{r}} \cdot \mathbf{T} = y_{2,l}\mathbf{P}_{lm} + ry_{4,l}\mathbf{B}_{lm} - y_{8,l}\mathbf{C}_{lm}$$

and $y_{6,l} = \dot{y}_{5,l} - 4\pi G\rho y_{1,l}$ $(B = \dot{P} + 4\pi G\rho U + (l+1)r^{-1}P)$

y_i system for degrees n different from 0 and 1:

$$
\begin{aligned}
\dot{y}_1 &= -\frac{2\lambda}{\lambda+2\mu}\frac{y_1}{r} + \frac{1}{\lambda+2\mu}y_2 + \frac{\lambda n(n+1)}{\lambda+2\mu}\frac{y_3}{r} \\
\dot{y}_2 &= \left[-4\rho g + \frac{4\mu(3\lambda+2\mu)}{(\lambda+2\mu)r}\right]\frac{y_1}{r} - \frac{4\mu}{\lambda+2\mu}\frac{y_2}{r} + n(n+1)\left[\rho g - \frac{2\mu(3\lambda+2\mu)}{(\lambda+2\mu)r}\right]\frac{y_3}{r} \\
&\qquad + \frac{n(n+1)}{r}y_4 - \rho y_6 \\
\dot{y}_3 &= -\frac{y_1}{r} + \frac{y_3}{r} + \frac{y_4}{\mu} \\
\dot{y}_4 &= \left[\rho g - \frac{2\mu(3\lambda+2\mu)}{(\lambda+2\mu)r}\right]\frac{y_1}{r} - \frac{\lambda}{\lambda+2\mu}\frac{y_2}{r} + \frac{2\mu\left[\lambda(2n^2+2n-1)+2\mu(n^2+n-1)\right]}{(\lambda+2\mu)r}\frac{y_3}{r} \\
&\qquad - \frac{3}{r}y_4 - \frac{\rho}{r}y_5 \\
\dot{y}_5 &= 4\pi G\rho y_1 + y_6 \\
\dot{y}_6 &= -4\pi G\rho n(n+1)\frac{y_3}{r} + \frac{n(n+1)}{r}\frac{y_5}{r} - \frac{2y_6}{r} \\
\dot{y}_7 &= \frac{y_7}{r} + \frac{y_8}{\mu} \\
\dot{y}_8 &= \frac{\mu(n^2+n-2)}{r}\frac{y_7}{r} - \frac{3y_8}{r}
\end{aligned}
$$

$\dot{y}_i(r) = c_{i,j}\,y_j(r)$ with $i,j = 1...6$: spheroidal system,
$\dot{y}_i(r) = c_{i,j}\,y_j(r)$ with $i,j = 7...8$: toroidal system.

Table of Contents

Spheroidal and toroidal modes

1/ Scalar equations and boundary conditions that determine U, V and P are decoupled from those that determine W

$\rightarrow$ a SNREI Earth model has two types of normal modes:

- *spheroidal* modes with displacements of the form $U\mathbf{P}_{lm} + V\mathbf{B}_{lm}$
- *toroidal* modes with displacements of the form $W\mathbf{C}_{lm}$

• *Spheroidal* oscillations **alter the external shape and internal density** of the Earth, hence they are accompagnied by perturbations $P\mathcal{Y}_{lm}$ in the gravitationnal potential

• *Toroidal* oscillations have **purely tangential** displacements and zero divergence: they leave the shape and the radial density distribution ρ of the Earth unaffected

Spheroidal and toroidal modes

2/ No dependence upon the azimuthal order $m \rightarrow$ every eigenfrequency is *degenerate* with an associated $(2l+1)$-dimensional eigenspace. This $2l+1$ degeneracy is a mathematical consequence of the spherical symmetry of the model.

3/ For each degree l there is an infinite number of spheroidal and toroidal modes: we need to introduce the *overtone number* $n = 0, 1, 2, ...$ We use index notation such as ${}_n\omega_l$ and ${}_nU_l, {}_nV_l, {}_nW_l$ to identify a particular eigenfrequency or eigenfunction.

Spheroidal and toroidal modes

4/ The $2l+1$ oscillations associated with a given eigenfrequency ${}_n\omega_l$ are referred to as a *multiplet*, designed by ${}_nS_l$ for spheroidal modes and by ${}_nT_l$ for toroidal modes.

5/ Each spheroidal eigenfunction ${}_nU_l\mathbf{P}_{lm} + {}_nV_l\mathbf{B}_{lm}$ within a multiplet ${}_nS_l$ and each toroidal eigenfunction ${}_nW_l\mathbf{C}_{lm}$ within a multiplet ${}_nT_l$ is referred to as a *singlet*.

6/ The lowest-frequency multiplet ${}_0S_l$ or ${}_0T_l$ is the *fundamental mode*. The next multiplet ${}_1S_l$ or ${}_1T_l$ is the first *overtone* and so on.

History

- Benioff (1958) reported the 1st evidence for a 57-min oscillation in the Pasadena electromagnetic strainmeter recording of the 1952 Kamchatka earthquake ($M_w 9$)

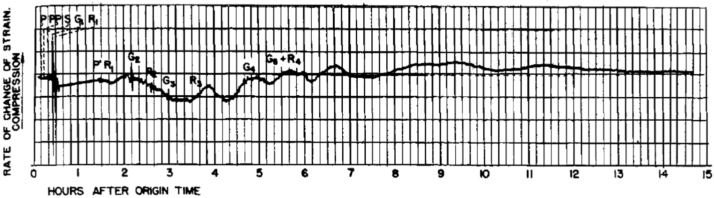

Fig. 8--Seismogram of Kamchatka earthquake, November 4, 1952, recorded by Benioff strain seismograph at Pasadena, drafted with 22 fold reduced recording rate

History

- strainmeter recording at Isabella, California, for the 1960 Chilean earthquake (M_w=9.5): one of the three records for the first observations of free oscillations of the Earth

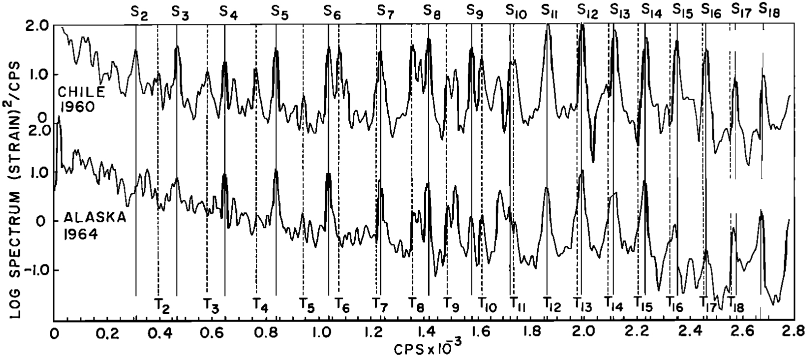

Fig. 4. Comparison of Chilean and Alaskan earthquake. Record length, 7854 min beginning 285 min after origin time for both events; sample interval, 3 min; bandwidth, $180{,}000^{-1}$ cps.

Smith (1966)
7854 min = 5.45 days

Toroidal modes: first-order radial equations

The toroidal oscillations of a SNREI Earth model have tangential displacement and traction vectors of the form

$$\mathbf{s} = W\mathbf{C}_{lm}, \qquad \vec{\mathbf{r}} \cdot \mathbf{T} = T\mathbf{C}_{lm}, \tag{9}$$

where $T = \mu\left(\dot{W} - r^{-1}W\right)$ and $\mathbf{C}_{lm} = k^{-1}\left[\vec{\boldsymbol{\theta}}\,(\sin\theta)^{-1}\,\partial_\phi - \vec{\boldsymbol{\Phi}}\partial_\theta\right]\mathcal{Y}_{lm}$.

$$\dot{W} = r^{-1}W + \mu^{-1}T, \, \dot{T} = \left[-\omega^2\rho + (k^2 - 2)\mu r^{-2}\right]W - 3r^{-1}T. \tag{10}$$

Both displacement and traction must be continuous across solid-solid discontinuities: $[W]_-^+ = 0$ and $[T]_-^+ = 0$ on $r = d_{SS}$. Tangential slip is allowed on the fluid-solid boundaries, but traction must vanish there and on the outer free surface: $T = 0$ on $r = d_{FS}$ and $r = a$.

- **no dependence upon incompressibility** κ (pure-shear nature of toroidal deformation)

Toroidal modes

The singlets have motions with l nodal planes on the surface.
$m = 0$

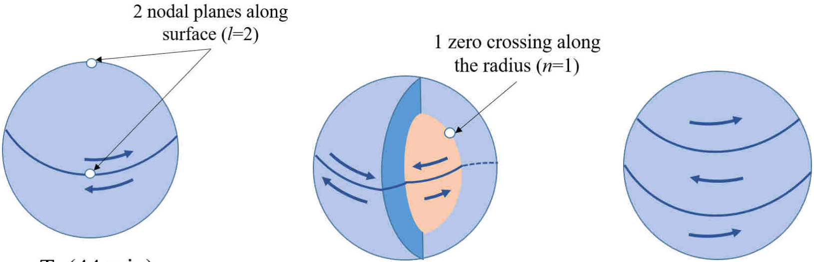

$_0T_2$ (44 min) « twist mode »

$_1T_2$ (12.6 min)

$_0T_3$ (28.4 min)

Note that $_0T_1$ **cannot exist** because it would require a twist back and forth of the entire sphere (net rotation), which contradicts the conservation of angular momentum for a rotating Earth.

Toroidal modes

$m = 0$ $\qquad$ $m = 1$ $\qquad$ $m = 2$

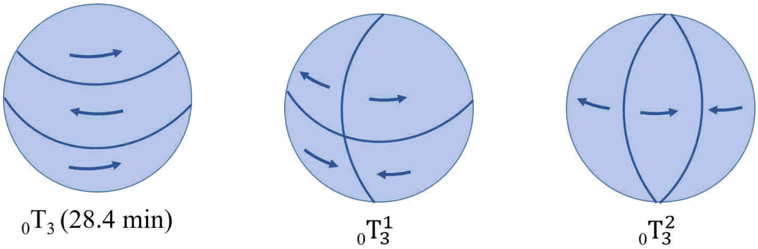

The azimuthal order $|m|$ counts the number of nodal surfaces in the longitudinal direction $\vec{\boldsymbol{\phi}}$. $|l - m|$ counts the number of nodal surfaces in the colatitudinal direction $\vec{\boldsymbol{\theta}}$.

Toroidal modes

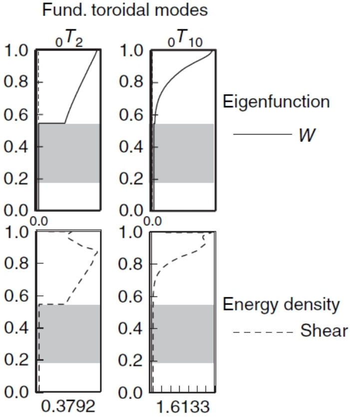

mHz

[Widmer-Schnidrig & Laske (2007). Normal Modes and Surface Wave Measurements, in: *Treatise on Geophysics*]

Displacements eigenfunctions ${}_nW_l$ and shear energy densities of some fundamental toroidal modes.

Toroidal modes are sensitive only to μ.

Sensitivity of a mode to structure with depth is not the eigenfunction but the *energy density*.

Energy density

- Total integrated energy of a normal mode of oscillation = kinetic energy + elastic-gravitational potential energy

- The potential energy can be decomposed into separate elastic *compressional*, elastic *shear* and *gravitational energies*.

$$\nu_\kappa = \int_V \kappa(\boldsymbol{\nabla}\cdot\mathbf{s})^2\,dV,$$

$$\nu_\mu = \int_V 2\mu(\mathbf{d}:\mathbf{d})\,dV,$$

where $\mathbf{d} = \frac{1}{2}[\boldsymbol{\nabla}\mathbf{s} + (\boldsymbol{\nabla}\mathbf{s})^T] - \frac{1}{3}(\boldsymbol{\nabla}\cdot\mathbf{s})\mathbf{I}$ is the deviatoric strain.

$$\nu_g = \int_V \rho\left[4\pi G\rho s_r^2 + \mathbf{s}\cdot\boldsymbol{\nabla}\phi + g(\mathbf{s}\cdot\boldsymbol{\nabla}s_r - s_r\boldsymbol{\nabla}\cdot\mathbf{s} - 2r^{-1}s_r^2)\right]dV$$

Toroidal modes

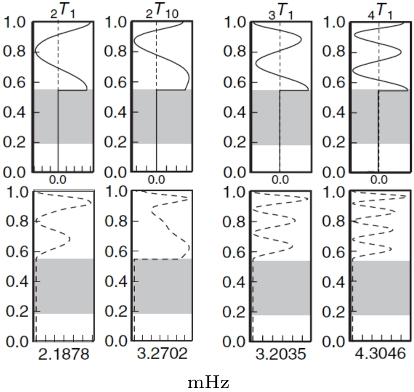

[Widmer-Schnidrig & Laske (2007). Normal Modes and Surface Wave Measurements, in: *Treatise on Geophysics*]

Displacements eigenfunctions $_nW_l$ and shear energy densities of some toroidal modes.

Toroidal modes are sensitive only to μ.

The overtone number n indexes the modes with increasing frequency and counts the number of nodal spheres. n : number of nodes in W

Toroidal modes

Remarks:

- The toroidal modes ${}_0T_l$, ${}_1T_l$, ${}_2T_l$, etc. correspond in the limit $l \gg 1$ to fundamental and higher-overtone *Love surface waves* or, equivalently, to constructively interfering **SH body waves** that turn into the upper mantle and are reflected beneath the seafloor.

- The depth to which a mode ${}_0T_l$, ${}_1T_l$, ${}_2T_l$ penetrates into the mantle decreases as the angular order l increases along the fundamental and each overtone branch n.

- Toroidal modes cannot be observed on vertical instruments for a SNREI Earth's model.

Spheroidal modes

$m = 0$

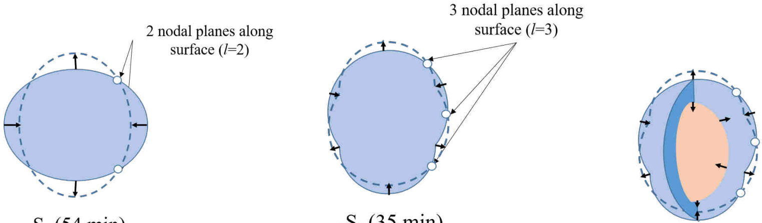

$_0S_2$ (54 min)
« football mode »

$_0S_3$ (35 min)
Pear-shaped mode

$_1S_3$ (18 min)

Note that $_0S_1$ **cannot exist** because it requires the displacement of the center of gravity of the Earth.

Spheroidal modes

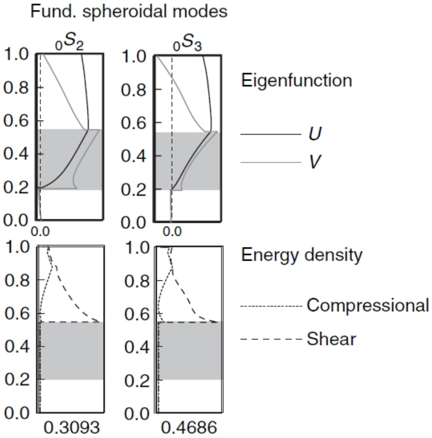

mHz

[Widmer-Schnidrig & Laske (2007). Normal Modes and Surface Wave Measurements, in: *Treatise on Geophysics*]

Eigenfunctions U and V and compressional shear energy densities for some fundamental spheroidal modes.

Spheroidal fundamental modes are not very sensitive to κ and μ in the core.

Spheroidal modes

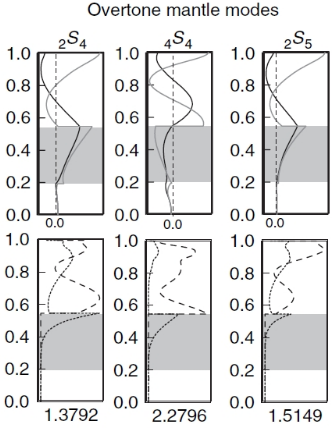

mHz

[Widmer-Schnidrig & Laske (2007). Normal Modes and Surface Wave Measurements, in: *Treatise on Geophysics*]

Eigenfunctions U and V and compressional shear energy densities for some overtone mantle modes.

Overtone mantle modes that are primarily sensitive to mantle structure are also influenced by κ in the core.

Spheroidal modes

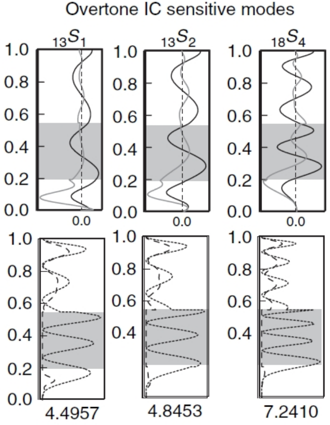

mHz

[Widmer-Schnidrig & Laske (2007). Normal Modes and Surface Wave Measurements, in: *Treatise on Geophysics*]

Eigenfunctions U and V and compressional shear energy densities for some inner core sensitive modes.

IC sensitive modes that can be observed at the Earth's surface are typically quite sensitive to mantle structure.

Stoneley modes

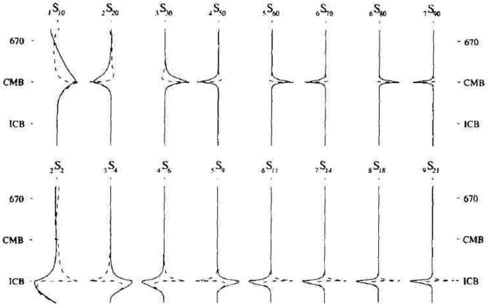

Figure 8.15. Eigenfunctions ${}_nU_l$ (*solid line*) and ${}_nV_l$ (*dashed line*) of a number of core-mantle boundary (CMB) Stoneley modes (*top row*) and inner-core boundary (ICB) Stoneley modes (*bottom row*). Vertical axis extends from the free surface to the center of the Earth.

[Dahlen & Tromp (1998)]

Modes that are confined in solid-fluid interfaces such as the CMB or ICB

CMB Stoneley modes

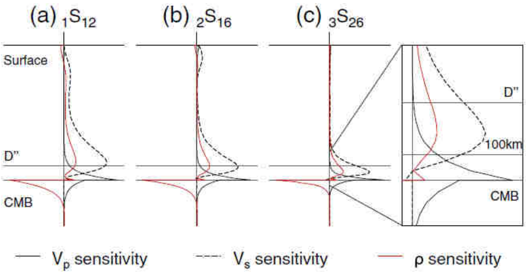

Figure 1. Sensitivity kernels for V_p (solid), V_s (dashed), and ρ (red) for representative CMB Stoneley modes $_nS_l$ and a zoom of the sensitivity in the D" region. Note that the Stoneley mode sensitivity becomes more focused at the CMB with increasing angular order l.

Modes that involve P-SV motion [Koelemeijer et al. (2013)]

Spheroidal mode: ${}_1S_1$

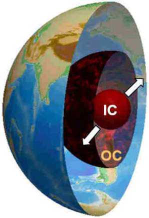

The so-called "Slichter" triplet
(Slichter 1960)

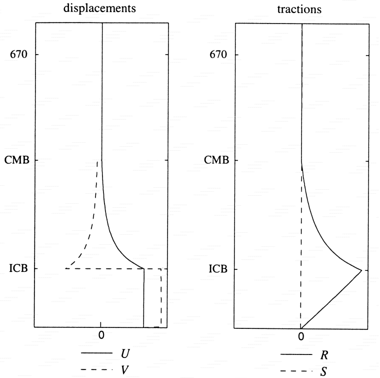

- feedback mechanism is Archimedean → **gravity** mode
- period ≈ 5.42 h → **sub-seismic** mode
- Never observed
- surface amplitude < 1 nGal ($10^{-12}g$)
- IC displacement < 1 mm

Radial modes

Radial modes have $l = 0,\ V = W = 0$.

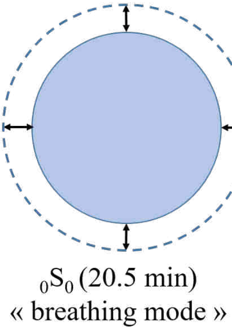

Radial modes

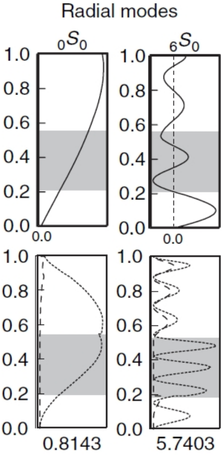

mHz

[Widmer-Schnidrig & Laske (2007). Normal Modes and Surface Wave Measurements, in: *Treatise on Geophysics*]

Eigenfunction U and compressional shear energy densities for some radial modes.

History

- Rigidity of the Inner Core inferred from normal mode observations

Table 1 Observed Normal Modes of the Earth sensitive to the Structure of the Inner Core

				UTD124B′—Solid inner core				UTD124B′—Liquid inner core		5.08M		HB_1	
						Inner core energy							
Mode	Mean period (s)	No. of obser-vations	s.e.m. (s)	Comp. period	Rel. error (%)	Compr.	Shear	Comp. period	Rel. error (%)	Comp. period	Rel. error (%)	Comp. period	Rel. error (%)
$_1S_0$	613.57	11	0.236	614.59	0.17	0.181	0.000	607.39	−1.02	610.06	−0.57	607.4	−1.01
$_2S_0$	398.54	40	0.084	397.59	−0.24	0.206	0.001	392.31	−1.59	391.42	−1.81	394.0	−1.14
$_3S_0$	305.84	7	0.129	306.00	0.05	0.233	0.003	301.36	−1.48	301.84	−1.31	300.9	−1.62
$_4S_0$	243.59	12	0.067	243.80	0.09	0.192	0.007	241.11	−1.03	241.55	−0.84	239.9	−1.51
$_2S_2$	904.23	21	0.487	904.43	0.02	0.001	0.080	914.94	1.17	917.80	1.50	915.1	1.20
$_5S_2$	397.36	11	0.157	397.03	−0.09	0.015	0.102	399.93	0.67	398.20	0.21	399.1	0.44
$_6S_1$	348.41	21	0.046	348.23	−0.05	0.068	0.011	347.10	−0.38	347.38	−0.30	346.6	−0.52
$_7S_3$	281.37	11	0.113	281.59	0.08	0.004	0.022	282.77	0.50	283.34	0.70	282.1	0.22
$_8S_1$	272.10	11	0.144	271.79	−0.11	0.115	0.052	271.00	−0.40	270.92	−0.43	270.5	−0.59
	Nine modes—r.m.s.				0.12				1.01		1.00		1.02

Dziewonski & Gilbert (1971)

Spheroidal modes

The spheroidal modes ${}_0S_l$, ${}_1S_l$, ${}_2S_l$, etc. correspond in the limit $l \gg 1$ to fundamental and higher-overtone *Rayleigh surface waves* or, equivalently, to constructively interfering multiply reflected P and SV body waves that turn in the upper mantle.

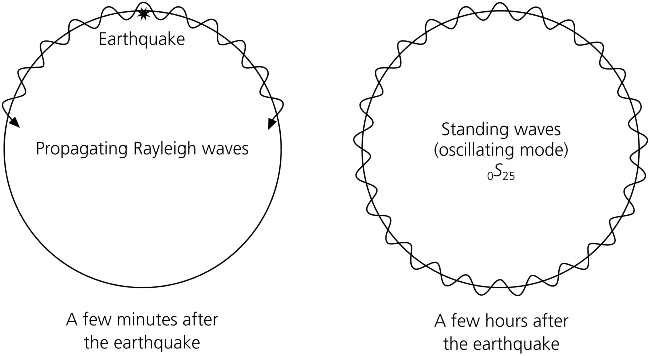

[from Stein & Wysession]

Spheroidal and toroidal modes

Animation:
https://saviot.cnrs.fr/terre/

Table of Contents

A very important point of normal mode theory is that the **basis of eigenfunctions is complete**: any displacement at the surface of the Earth can be expressed as a linear combination of the eigenfunctions

$$\mathbf{s}(\mathbf{r},t) = \Re \sum_k a_k \mathbf{s}_k(\mathbf{r}) e^{i\,{}_n\omega_l^m t}$$

where a_k depends on forcing, $\mathbf{s}_k(\mathbf{r}) = {}_n\mathbf{s}_l^m(\mathbf{r})$ are written as

$$\begin{aligned} {}_n\mathbf{s}_l^m(\mathbf{r}) = \Big(& \underbrace{\vec{\mathbf{r}}\,{}_nU_l(r)\mathcal{Y}_l^m(\theta,\phi) + k^{-1}\,{}_nV_l(r)\boldsymbol{\nabla}_1\mathcal{Y}_l^m(\theta,\phi)}_{\text{spheroidal mode}} \\ & - \underbrace{k^{-1}\,{}_nW_l(r)\vec{\mathbf{r}} \times \boldsymbol{\nabla}_1\mathcal{Y}_l^m(\theta,\phi)}_{\text{toroidal mode}} \Big) \end{aligned} \tag{11}$$

with radial eigenfunctions, spherical harmonics and eigenfrequencies.

Green tensor

The response of the Earth to any forcing (e.g. earthquake, surface load) which excites its free oscillations (and the equivalent travelling body and surface waves) can be expressed in terms of the second-order *Green tensor* or *impulse response* $\mathbf{G}(\mathbf{x},\mathbf{x}';t)$: displacement response at $\mathbf{x}$, t to a unit impulsive force acting at $\mathbf{x}'$, $t=0$.

$\mathbf{G}$ is solution to the homogeneous equation

$$\rho^0(\partial_t^2\mathbf{G}+\mathcal{H}\mathbf{G})=\mathbf{0},$$

where $\mathcal{H}$ is the gravito-elastic linear operator and subject to initial conditions $\mathbf{G}(\mathbf{x},\mathbf{x}';0)=\mathbf{0}, \partial_t\mathbf{G}(\mathbf{x},\mathbf{x}';0)=(1/\rho^0)\mathbf{I}\delta(\mathbf{x}-\mathbf{x}')$.

The impulse response $\mathbf{G}$ is written

$$\boxed{\mathbf{G}(\mathbf{x},\mathbf{x}';t)=\Re\sum_k(i\omega_k)^{-1}\mathbf{s}_k(\mathbf{x})\mathbf{s}_k(\mathbf{x}')e^{i\omega_k t},\ \text{for}\ t\geq 0}$$

Green tensor

Remarks:

- since $\mathbf{s}_k$ are real, the phase of every oscillation is the same ($\pm\pi$) throughout the Earth: characteristic of a *standing wave*.
- $\mathbf{G}$ is symmetric: $\mathbf{G}(\mathbf{x}, \mathbf{x}'; t) = \mathbf{G}^T(\mathbf{x}', \mathbf{x}; t)$ *principle of seismic reciprocity*. (NB: when the Earth is rotating, not true any more: *principle of anti-Earth* needed)

The displacement produced by any body force density $\mathbf{f}$ and surface force density $\mathbf{t}$ is the convolution of the impulse response $\mathbf{G}$ with the entire past history of the forces

$$\begin{aligned} \mathbf{s}(\mathbf{x}, t) = & \int_{-\infty}^{t} \int_{V} \mathbf{G}(\mathbf{x}, \mathbf{x}'; t - t') \cdot \mathbf{f}(\mathbf{x}', t')\, dV'\, dt' \\ & + \int_{-\infty}^{t} \int_{S} \mathbf{G}(\mathbf{r}, \mathbf{x}'; t - t') \cdot \mathbf{t}(\mathbf{x}', t')\, d\Sigma'\, dt' \end{aligned} \tag{12}$$

This embodies the *principles of superposition and causality*.

The "Hum" or continuous background free oscillations

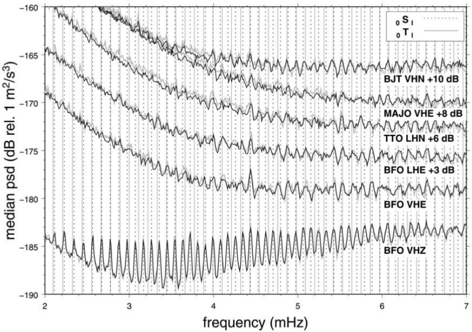

Figure 1. Comparison of median power spectral densities of the 1000 least noisy time windows from each of the sensors. For clarity, the spectra have been vertically shifted. Vertical lines mark the frequencies of fundamental spheroidal and toroidal modes. The underlying gray spectra were computed after the rejection of time windows affected by earthquakes with $M_W \geq 5.5$.

[Kurrle & Widmer-Schnidrig (2008)]

- permanent excitation of fundamental spheroidal (Rayleigh waves) and toroidal (Love waves) modes
- most likely excitation mechanism: coupling between ocean infragravity waves and seismic surface waves through seafloor topography + atmospheric pressure [Nishida 2014]

Gravitational waves

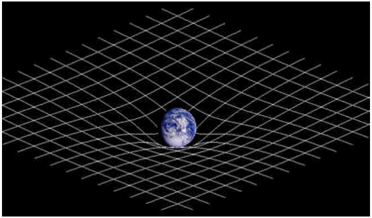

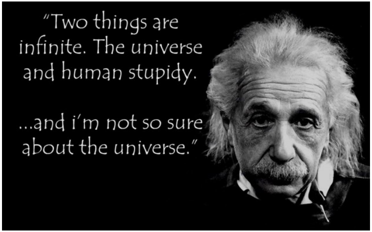

- mass $\rightarrow$ space curvature
- moving mass $\rightarrow$ displacement of this curvature $\rightarrow$ GWs (*ripples* in space-time)
- variation of distance between 2 masses
- GWs have a weak amplitude (relative variation between 10^{-12} - 10^{-20} m, proton size $\sim 10^{-15}$ m), but poor interaction with masses $\rightarrow$ information on generating sources

Gravitational waves

Exaggerated effects of GWs on Earth (Credit: LIGO/R. Hurt, Caltech/MIT/LIGO Lab)

Gravitational waves

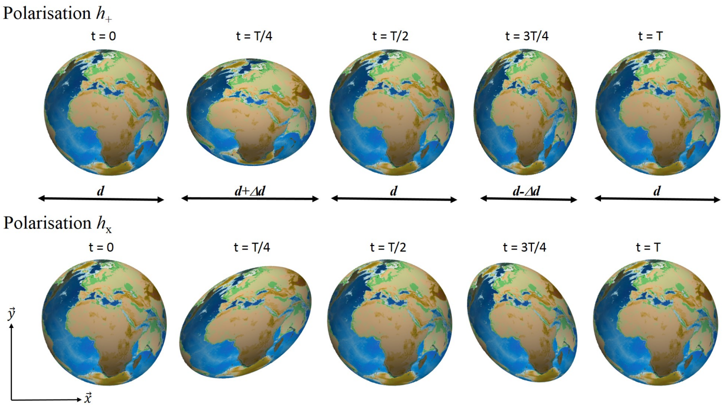

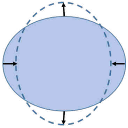

${}_0S_2$

Gravitational waves

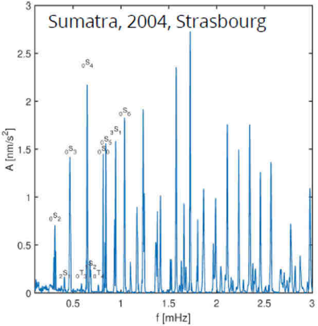

$$\mathbf{f}(\mathbf{r},t) = -\frac{\partial \mu}{\partial r}\mathbf{e}_r \cdot \underbrace{\mathbf{h}(\mathbf{r},t)}_{\text{metric perturbation}}$$

[Dyson (1969)]

$1\ \mathrm{nm/s^2} \sim 10^{-2}\ \mathrm{cm}$

Binary white-dwarfs ($h_0 \sim 10^{-22} \rightarrow 10^{-10}$ cm)

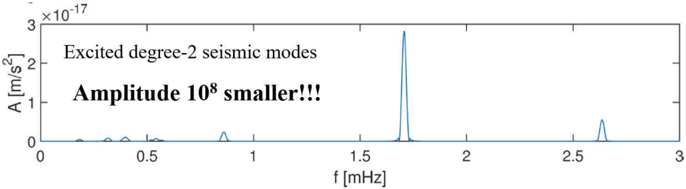

[Majstorovic et al. (2019)]

Table of Contents

Splitting and coupling

- Any departure of the Earth model from spherical symmetry removes the eigenfrequency degeneracy and causes the multiplets ${}_nS_l$ and ${}_nT_l$ to *split* (into $2l + 1$ frequencies) and *couple* (transfer of energy).

- The principal deviations from the spherically symmetric reference state are Earth's daily **rotation**, its hydrostatic **ellipticity** in response to the rotation and general **aspherical structure** (topography of interfaces, lateral variations in volumetric parameters).

Mode splitting and coupling

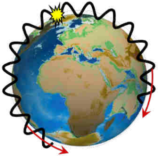

Rotation (Coriolis)

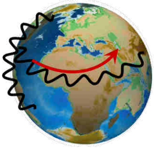

Waves in the direction of rotation travel faster

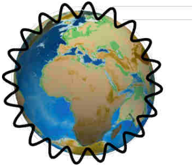

Ellipticity

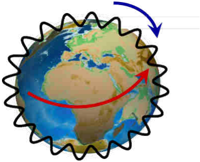

Waves from pole to pole run a shorter path (67 km) than along the equator

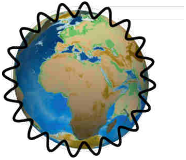

3D

Waves slowed down (or accelerated) by heterogeneities

First-order Coriolis splitting

We ignore the centrifugal potential and associated ellipticity perturbation.

χ is the *Coriolis splitting parameter*

$$\chi = k^{-2} \int_0^a \rho(V^2 + 2kUV + W^2) r^2 \, dr, \text{ where } k = \sqrt{l(l+1)}.$$

First-order Coriolis splitting is analogous to the *Zeeman splitting* of the quantum energy levels of a hydrogen atom in a magnetic field.

The eigenfrequency of the m^{th} singlet within a k^{th} multiplet on a rotating Earth in hydrostatic equilibrium is given

$$\omega_k^m = \overline{\omega}_k + m\chi\Omega \text{ with } -l \leq m \leq l$$

First-order Coriolis splitting

- The eigenfrequency perturbations are *uniformly spaced.*

- For toroidal modes ${}_nT_l$, $\int_0^a \rho W^2 r^2 dr = 1$ implies that $\chi = [l(l+1)]^{-1}$, then $\omega_k^m = \overline{\omega}_k - \frac{m}{l(l+1)}\Omega$ with $-l \leq m \leq l$

- Radial modes ${}_nS_0$ (since they are non-degenerate) are unaffected by Coriolis force to first order in $\Omega/\overline{\omega}_k$.

- First-order Coriolis splitting dominates for low-frequency seismic modes (below 1 mHz).

Rotational splitting: History

- Double-peak ${}_0S_2$ and ${}_0S_3$ modes after 1960 Chile earthquake explained as rotational splitting by Backus & Gilbert (1961) and Pekeris et al. (1961)

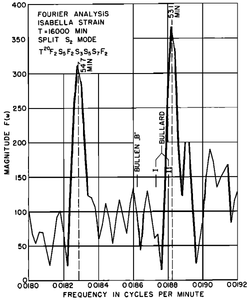

Fig. 2. High resolution Fourier analysis of Isabella strain seismograms to show split spectral peak. Filter $T^{20}F_2S_5F_2S_3S_5S_7F_2$, record length 16,000 minutes.

Benioff et al. (1961)

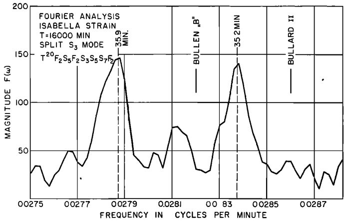

Fig. 3. High resolution Fourier analysis of Isabella strain seismograms to show split spectral peak. Filter $T^{20}F_2S_5F_2S_3S_5S_7F_2$, record length 16,000 minutes.

16000 min = 11.1 days

- Unbeknownst to them, the rotational splitting had been investigated by Cowling & Newing (1949) and Ledoux (1951) in an astrophysical context.

First-order Coriolis splitting

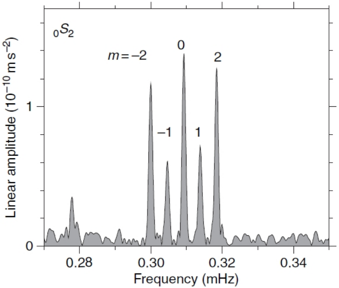

Example: Zeeman splitting of $_0S_2$. Fourier amplitude spectrum of a 500 h long record of the 2004 M_w9.3 Sumatra event by the superconducting gravimeter at Strasbourg, France.

[Rosat et al. (2005)]

Example: Zeeman splitting of $_0S_3$. Fourier amplitude spectrum of a 600 h long record of the 2004 M_w9.3 Sumatra event by the superconducting gravimeter at Sutherland.

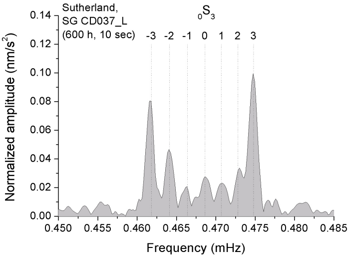

Splitting due to rotation and ellipticity

Combined effects of **rotation and hydrostatic ellipticity**.

$$\omega_k^m = \overline{\omega}_k \left(1 + a + bm + cm^2\right) \text{ with } -l \leq m \leq l,$$

where $\overline{\omega}_k$ is the multiplet degenerate frequency, a and c the ellipticity splitting coefficients and b the rotational splitting coefficient.

$\overline{\Psi} = \frac{1}{3}\Omega^2 r^2$: centrifugal potential

$$a = \frac{1}{3}\underbrace{(1 - k^2\chi)(\Omega/\overline{\omega}_k)^2}_{\text{spherical part of } \overline{\Psi}} + \underbrace{\frac{1}{2}\overline{\omega}_k^{-2}(\nu - \overline{\omega}_k^2\tau)}_{\substack{\text{degree-2 perturbations} \\ \text{in } \overline{\Psi} \text{ and ellipticity}}} ,$$

$$b = \chi(\Omega/\overline{\omega}_k), \; c = -\frac{3}{2}\overline{\omega}_k^{-2}k^{-2}(\nu - \overline{\omega}_k^2\tau)$$

ν and τ depends on ellipticity, density, incompressibility and rigidity.

Splitting due to rotation and ellipticity

- Shift in the mean frequency of the multiplet:

$$\frac{1}{2l+1}\sum_m \delta\omega_m = \frac{1}{3}(1 - k^2\chi)(\Omega^2/\overline{\omega}_k)$$

- A toroidal multiplet ${}_nT_l$ does not exhibit any net shift $(k^2\chi = 1)$

- Every radial mode eigenfrequency is increased by an amount $\overline{\omega}_k \rightarrow \overline{\omega}_k \left[1 + \frac{1}{3}(\Omega/\overline{\omega}_k)^2\right]$

Splitting due to rotation and ellipticity

- splitting due to ellipticity is **asymmetric** wrt degenerate frequency
- ellipticity removes the degeneracy only partly: $\omega_k^m = \overline{\omega}_k \left(1 + a + cm^2\right)$
- rotational splitting is **symmetric** wrt degenerate frequency
- rotation removes the degeneracy completely
- Coriolis force exerts a perturbation of order $\Omega/\overline{\omega}_k$
- centrifugal force is a perturbation of order $(\Omega/\overline{\omega}_k)^2$
- rotation dominates at low frequencies ($b \gg c$)
- 2nd-order Coriolis splitting should be considered for a complete treatment of Earth's rotation

Coriolis coupling

- Coupling exists between modes
- Strength of coupling is larger for modes of nearby frequencies

  $\propto \sum_{k \neq 0} \frac{\omega_0^2}{\omega_0^2 - \omega_k^2} \left| \int_V \rho \mathbf{s}^*{}_k \cdot (i\Omega \times \mathbf{s}_0) \, dV \right|^2$

- Coriolis coupling is significant for several of the Earth's gravest modes (e.g. ${}_0T_2$)

Coriolis coupling

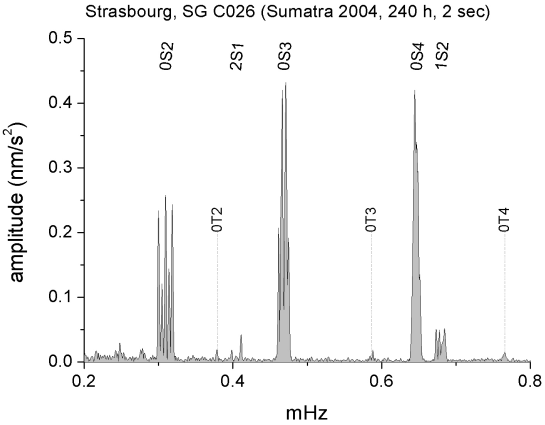

Coupling due to rotation and ellipticity

Selection rules for a rotating, elliptical but **laterally homogeneous** Earth:

- Coriolis force causes spheroidal-toroidal coupling between mode pairs of the form ${}_nS_l - {}_{n'}T_{l\pm1}$ and ${}_nT_l - {}_{n'}S_{l\pm1}$, that is between multiplets that differ by a *single* angular degree ($|l - l'| = 1$)
- Earth's ellipticity gives rise to spheroidal-toroidal coupling for $|l - l'| = 1$
- rotation causes spheroidal-spheroidal coupling for $|l - l'| = 0$ (pairs of *same* angular order)
- ellipticity causes same-type (spheroidal or toroidal) mode coupling for $|l - l'| = 0$ (i.e. pairs of the form ${}_nS_l - {}_{n'}S_l$ and ${}_nT_l - {}_{n'}T_l$ and for $|l - l'| = 2$ (i.e. pairs of the form ${}_nS_l - {}_{n'}S_{l\pm2}$ and ${}_nT_l - {}_{n'}T_{l\pm2}$

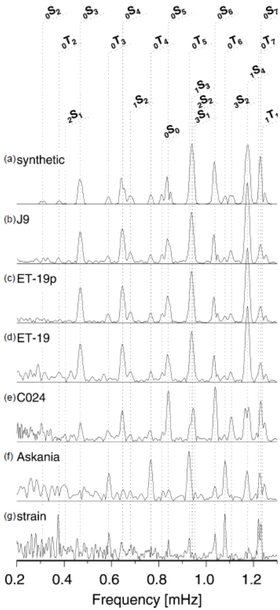

[Zürn et al. (2000)]

Amplitude spectra after 1998 $M_w 8.1$ Balleny Islands earthquake at BFO.

(a): synthetic (rotation, ellipticity and 3D-mantle model S16B30 (Masters et al. 1996)

(b): superconducting gravimeter at Strasbourg (France)

(c): Lacoste-Romberg ET19 gravimeter at BFO (pressure corrected)

(d): Lacoste-Romberg ET19 gravimeter at BFO (without pressure correction)

(e): superconducting gravimeter at Boulder (USA)

(f): borehole-tiltmeter at BFO

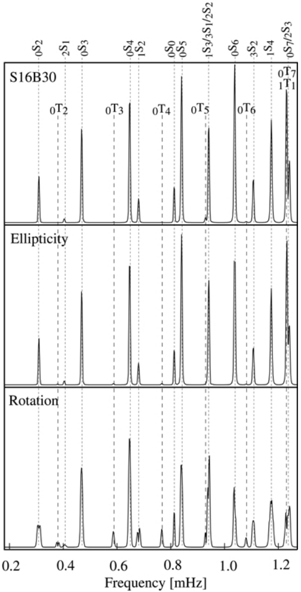

[Zürn et al. (2000)]

Synthetic spectra of 100-h long vertical acceleration computed for 1998 $M_w 8.1$ Balleny Islands earthquake at BFO.

Top: only 3D-mantle model S16B30 (Masters et al. 1996)

Middle: only ellipticity

Bottom: only rotation

Rotation is clearly the most effective mechanism for peaks to appear at toroidal mode frequencies.

Effect of lateral heterogeneities

$$\omega_k^m = \overline{\omega}_k \left(1 + a + bm + cm^2\right) + H^{\mathrm{lat}}_{mm'},$$

$$\text{with } H^{\mathrm{lat}}_{mm'} = \overline{\omega}_k \sum_{st} c_{st} \int_V \mathcal{Y}_{lm}\mathcal{Y}_{st}\mathcal{Y}_{l'm'}\, dV,$$

where c_{st} represent perturbations (beyond first-order ellipsoidal perturbations) in incompressibility, rigidity, density expanded in real surface spherical harmonics. s represents the degree of the heterogeneity.

The real *Gaunt integrals* satisfy the *selection rules*

$$\int_V \mathcal{Y}_{lm}\mathcal{Y}_{st}\mathcal{Y}_{l'm'}\, dV = 0 \text{ unless } \begin{cases} s \text{ is even} \\ 0 \leq s \leq 2l \\ t = m - m' \end{cases}$$

- the splitting of an isolated multiplet depends upon the **even-degree** structure of the Earth

Effect of lateral heterogeneities

$$\omega_k^m = \overline{\omega}_k \underbrace{\left(1 + a + bm + cm^2\right)}_{\text{rotation and ellipticity}} + \overline{\omega}_k \sum_{\substack{s=0 \\ s \text{ even}}}^{2l} \sum_{t=-s}^{s} \gamma_{ls}^{mm't} \underset{\substack{\downarrow \\ \text{lateral heterogeneities}}}{c_{st}} \tag{13}$$

We define the *splitting matrix* H such as

$$H_{mm'} = \overline{\omega}_k \left[\left(a + bm + cm^2\right) \delta_{mm'}\right] + \overline{\omega}_k \sum_{\substack{s=0 \\ s \text{ even}}}^{2l} \sum_{\substack{t=-s \\ t=m-m'}}^{s} \gamma_{ls}^{mm't} c_{st} + \text{anisotropy}$$

The matrix H is called *self-coupling matrix* with dimension $(2l+1)$ x $(2l+1)$ in this case of an *isolated multiplet*.

Effect of lateral heterogeneities

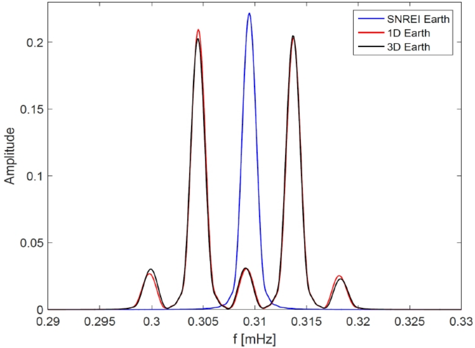

Predicted ${}_0S_2$ amplitude FFT spectrum

SNREI: spherically symmetric, non-rotating, perfectly elastic and isotropic Earth's model

1D Earth: consider splitting due to rotation and ellipticity

3D Earth: includes in addition the self-coupling due to lateral heterogeneity

Effect of lateral heterogeneities

Estimation of the second-order axisymmetric structure coefficient c_{20} for ${}_0S_2$ multiplet

Majstorovic et al. (2019) used long-period seismometer and Superconducting Gravimeter records
Häfner & Widmer-Schnidrig (2013) used Superconducting Gravimeter records

Multiplet coupling

In a rotating, elliptical, anelastic and heterogeneous Earth's model, coupling exists between multiplets.

The splitting matrix H is extended to dimension $\sum_k (2l_k + 1)$ x $\sum_k (2l_k + 1)$ where l_k denotes the degree of the multiplet k.

Synthetic seismogram computation:

- self-coupling: one multiplet considered isolated
- group coupling: chains of multiplets (e.g. ${}_0S_2 - {}_0T_2 - {}_2S_1 - {}_0S_3$, ${}_0T_5 - {}_2S_2 - {}_1S_3 - {}_3S_1$)
- full coupling (e.g. all 140 spheroidal and toroidal modes up to 3 mHz)

Effect of lateral heterogeneities

Selection rules for a non-rotating, spherical but **laterally heterogeneous** Earth:

- A multiplet ${}_nS_l$ or ${}_nT_l$ is coupled to a multiplet ${}_{n'}S_{l'}$ or ${}_{n'}T_{l'}$ by a lateral variation of degree s only if $|l - l'| \leq s \leq l + l'$

- Two spheroidal multiplets ${}_nS_l$ and ${}_{n'}S_{l'}$ are coupled by a lateral variation of degree s only if $l + l' + s$ is *even*

- Two toroidal multiplets ${}_nT_l$ and ${}_{n'}T_{l'}$ are coupled by a lateral variation of degree s only if $l + l' + s$ is *even*

- A spheroidal multiplet ${}_nS_l$ is coupled to a toroidal multiplet ${}_{n'}T_{l'}$ by a lateral variation of degree s only if $l + l' + s$ is *odd*

Effect of lateral heterogeneities

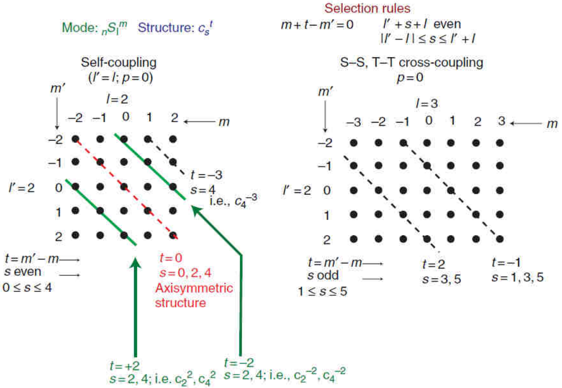

Figure 15 Elements in the splitting matrix that are affected by coupling. Left panel: An isolated $\ell=2$ mode experiences self-coupling through Earth's rotation and ellipticity. Together with axisymmetric structure this manifests itself in the diagonal. Other even-degree structure (s even) affects off-diagonal elements. When two modes couple, the splitting matrix has four blocks: two self-coupling blocks (one for each mode) and two cross-coupling blocks. The right panel shows how elements in a cross-coupling block with an $\ell'=3$ mode are affected for same-type coupling ($p=0$). Some of the elements are now affected by odd-degree structure (s odd).

[Widmer-Schnidrig & Laske (2007).
Normal Modes and Surface Wave Measurements, in: *Treatise on Geophysics*]

Example of multiplet coupling: ${}_0S_0$

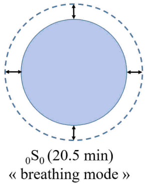

The circumference of the Earth gets bigger and the crust must get thinner. Amplitude variations of ${}_0S_0$ ($Q \approx 5000$) could be due to lateral variations of the Poisson ratio.

$$\nu = \frac{\text{thinning}}{\text{elongation}}$$

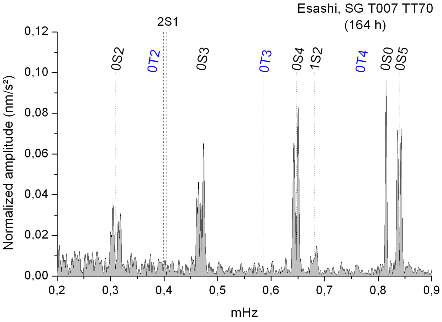

After 2004 M_w9.3 Sumatra-Andaman earthquake

Example of multiplet coupling: ${}_0S_0$

Ellipticity and rotation → 1% higher at the pole than at the equator (latitude dependency)

- Two spheroidal multiplets ${}_nS_l$ and ${}_{n'}S_{l'}$ are coupled by a lateral variation of degree s only if $l + l' + s$ is *even*

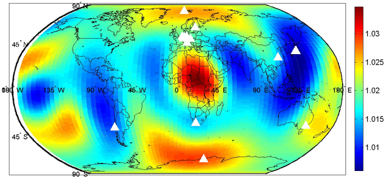

Predicted ${}_0S_0$ amplitude after 2004 $M_w 9.3$ Sumatra-Andaman event showing latitude and longitude dependency

[Rosat et al. (2007)]

→ Coupling between ${}_0S_0$ and ${}_0S_5$ through degree-5 structure coefficients

Multiplet coupling: synthetic seismogram computation

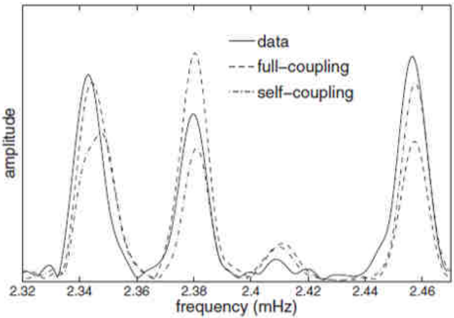

[Al-Attar et al. (2012)]

Splitting functions

Splitting function coefficients were introduced by Woodhouse et al. (1986) as a convenient way to describe the splitting of normal modes in a complete way.

These c_{st} are linearly dependent to the perturbations of the reference Earth model

$$c_{st} = \int_0^a \delta m_{st}(r) K_s(r) dr + \sum_d \delta h_{st}^d H_s^d,$$

where δm_{st} angular order s and azimuthal order t perturbations in S-wave velocity, P-wave velocity, density and anisotropy. δh_{st}^d represent topography on discontinuities d. $K_s(r)$ and H_s^d are associated sensitivity kernels (Woodhouse 1980).

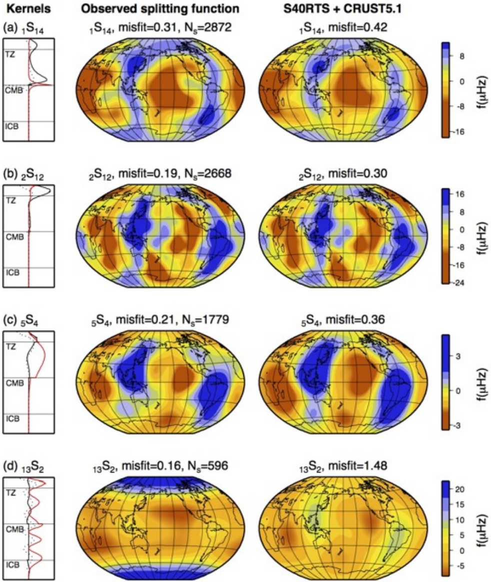

[Deuss et al. (2013)]

Observed splitting function maps and predictions for mantle model S20RTS.

These maps show the local variation in splitting due to the underlying heterogeneity.

N_s: total number of spectra used for the splitting function measurement.
Left panels: sensitive kernels (red is v_p, solid black is v_s, dashed is density).

Table of Contents

Conclusion

- Spheroidal modes ${}_nS_l$: volume change (alter shape and density distribution)
- Toroidal modes ${}_nT_l$: purely tangential displacements and divergent-free (do not alter shape and density)
- Rotation, ellipticity, lateral heterogeneities $\rightarrow$ remove the $2l+1$ degeneracy $\rightarrow$ **splitting and coupling** of modes
- Below 1 mHz, Coriolis coupling dominates and modes have strong sensitivity to **density**
- Coupling: toroidal modes can be observed on vertical instruments
- Frequency analysis of modes to retrieve **even** degree structure coefficients $\rightarrow$ Coupling between multiplets must be considered to retrieve **odd** degree structure coefficients $\rightarrow$ tomography models
- Seismic modes provide information about density but **trade-off with P-wave velocity structure** not solved yet (debate going on)
- Normal modes form a complete basis to compute Earth's deformation from various excitation sources

Backup slides

Orthonormality

V denotes the unit sphere. Real surface spherical harmonics are orthonormal.

$$\int_V \mathcal{Y}_{lm}\mathcal{Y}_{l'm'}\, dV = \int_V \mathbf{P}_{lm}\cdot\mathbf{P}_{l'm'}\, dV = \tag{14}$$
$$\int_V \mathbf{B}_{lm}\cdot\mathbf{B}_{l'm'}\, dV = \int_V \mathbf{C}_{lm}\cdot\mathbf{C}_{l'm'}\, dV = \delta_{ll'}\delta_{mm'}$$

The displacement eigenfunctions of a SNREI Earth model must satisfy the general orthonormality relation

$$\int_V \rho\ \mathbf{s}_k\cdot\mathbf{s}_{k'}\, dV = \delta_{kk'},$$

where k is used to identify a quadripartite $\{n, l, m; S \text{ or } T\}$. The spheroidal and toroidal eigenfunctions of different degree or order as well as spheroidal-toroidal pairs of eigenfunctions are orthogonal. The spheroidal and toroidal radial eigenfunctions *of the same degree* l must be orthonormal.

$$\int_0^a \rho\left({}_nU_l{}_n'U_l + {}_nV_l{}_n'V_l\right) r^2\, dr = \delta_{nn'},\ \int_0^a \rho\left({}_nW_l{}_n'W_l\right) r^2\, dr = \delta_{nn'} \tag{15}$$

Splitting and coupling of modes below 1 mHz

- high sensitivity to density heterogeneities (destabilizing effect of self-gravitation)
- frequency closer to the frequency of Earth's rotation leading to a pronounced Zeeman splitting
- Zeeman splitting depends on spherically averaged density structure: $\omega_k^m = \overline{\omega}_k\,(1 + bm)$ for $-l \leq m \leq l$

From measured ω_k^m, we can estimate b for a given multiplet k.

$$\frac{\overline{\omega}_k}{\Omega} b_k = k^{-2} \int_0^a \rho(V^2 + 2kUV + W^2) r^2 \, dr.$$

$\rightarrow$ linear constraints on the 1D density profile without any trade-off with elastic parameters [Zürn et al. 2000, Widmer-Schnidrig 2003]

Multiplet coupling: synthetic seismogram computation

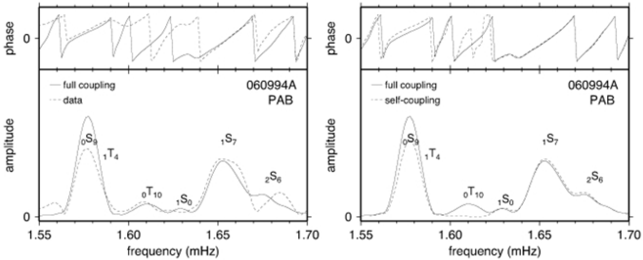

[Deuss & Woodhouse (2001)]

Normal mode spectrum at station PAB for the large $M_w 8.3$ and deep Bolivia event of 9 June 1994.

The differences between full- and self-coupling synthetics (right) are of the same order as the differences between the observed data and full-coupling synthetics (left).